

Electronic supplementary information

1. Actual device photograph and the modes of operation

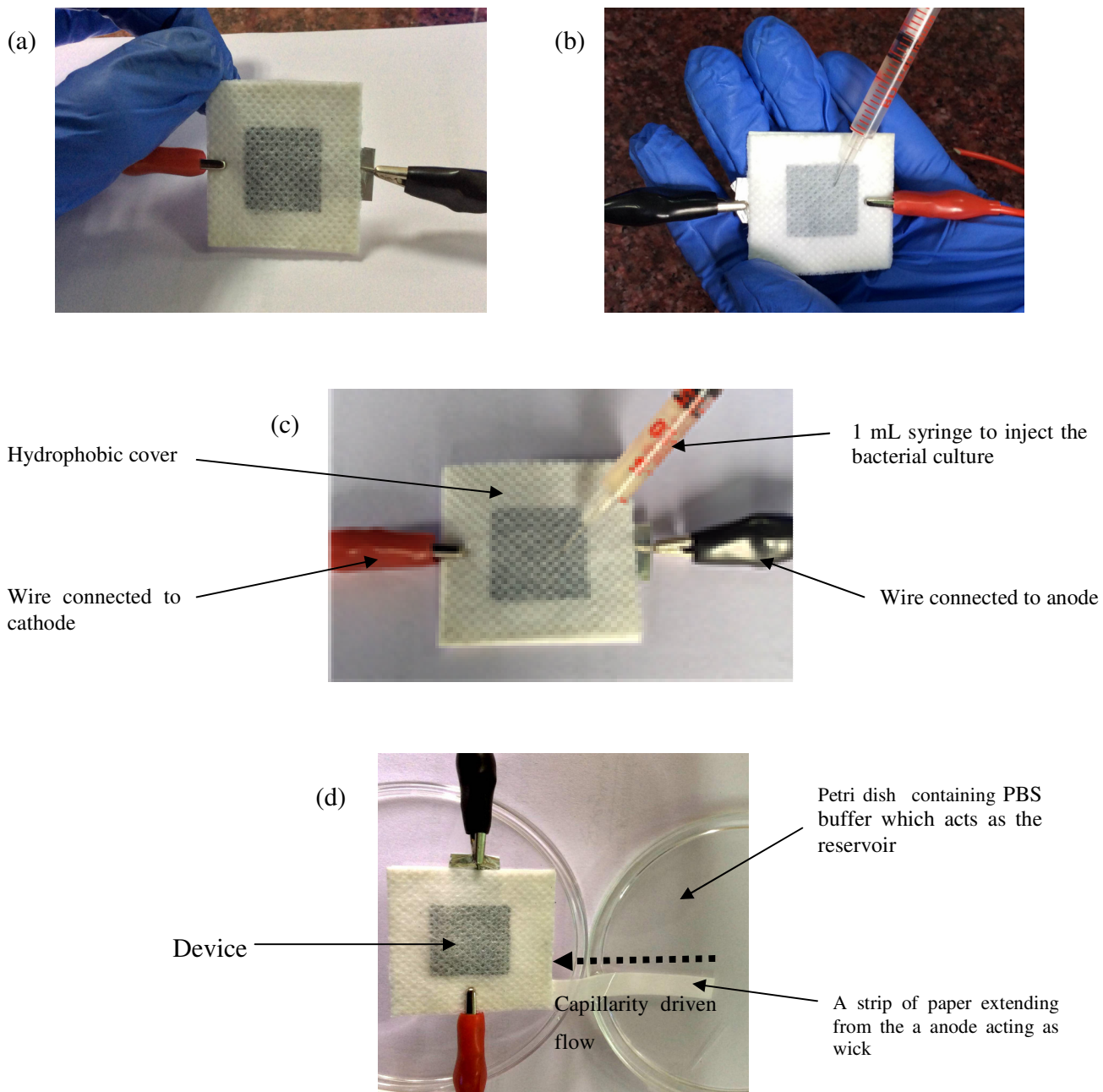


Figure S1: Pictures of the set-up operated in (a), (b), (c) batch mode and (d) continuous mode

2. Electron transfer mechanisms

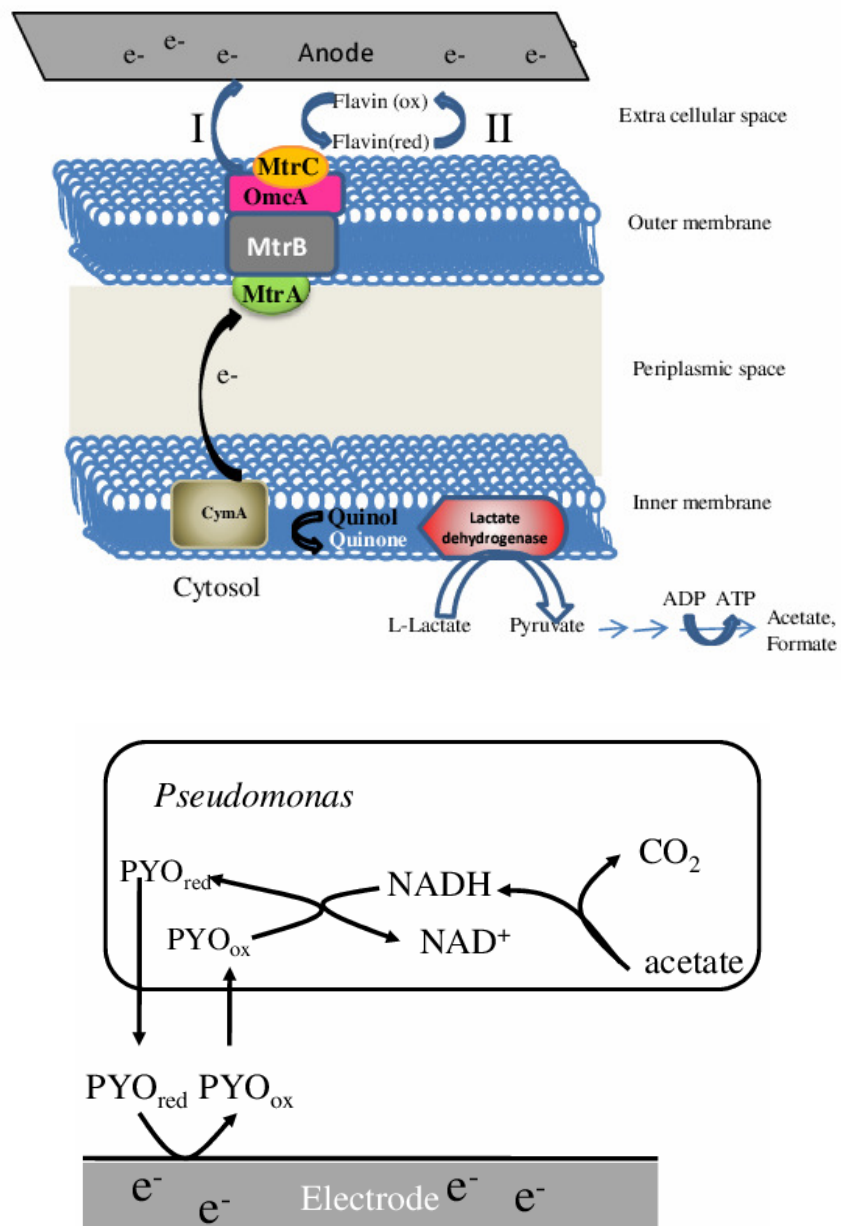


Figure S2: (a) Schematic of the Extracellular Electron Transport (EET) to anode occurring in *Shewanella putrificiens* and (b) *Pseudomonas aeruginosa*.

In exoelectrogens, the extracellular electron transfer is aided via the protein complexes in the cell membranes and by the means of the certain exogenous mediators which are secreted by the

bacteria into the media. These mediators (Pyocyanin(PYO) in case of *Pseudomonas aeruginosa* and flavins in case of *Shewanella putrificiens*) shuttle the electrons between cells and electrode carrying the electron by a series of oxidation and reduction reaction. The electrogenic potential of bacteria hence, depends not only upon the amount of bacteria adhered to the electrode but also on the concentration of these exogenous compounds.

3. X-ray diffraction analysis of the electrodes

X-ray diffraction analysis shows 5 peaks among which 1, 2, 3 and 5 correspond to the presence of various forms of cellulose (amorphous and crystalline) in the Whatman no. 1 filter paper; the sharp peak 4 (26.5°)¹⁻³ corresponds to pristine graphite. A clear difference in the peak intensity of graphite can be observed when different strokes are adopted, indicating the varying amounts of graphite in both anode and cathode.

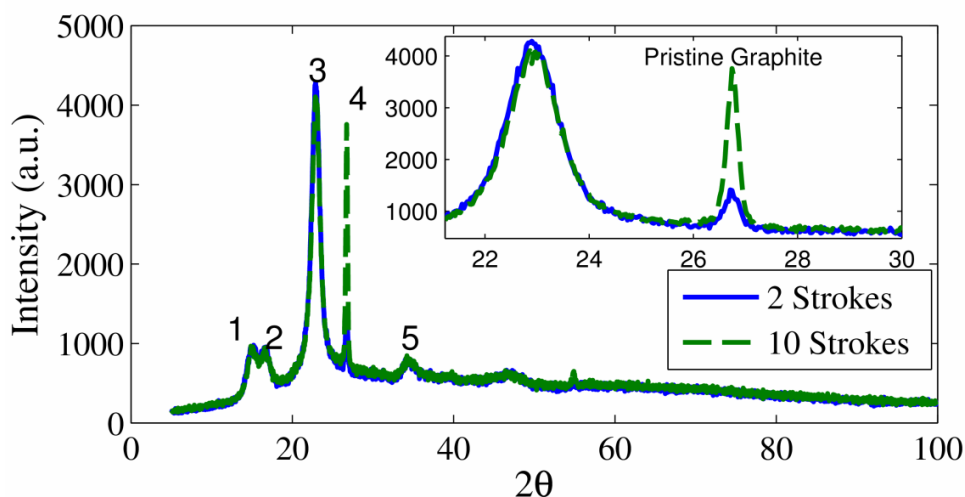


Figure S3: X-ray diffraction (XRD) analysis of anode (2 pencil strokes) and cathode (10 pencil strokes).

4. SEM analysis of the electrodes and bacteria

The surface morphology and composition are studied using Zeiss Supra scanning electron microscope at an accelerating voltage of 20 KV. The device is cut open and the anode is carefully removed from the device. Samples are pre-treated using 2 %v/v glutaraldehyde at 4°C

overnight to fix the bacteria on the surface of the paper matrix followed by the subsequent drying using increasing concentrations of alcohol (30 % to 70 %v/v).

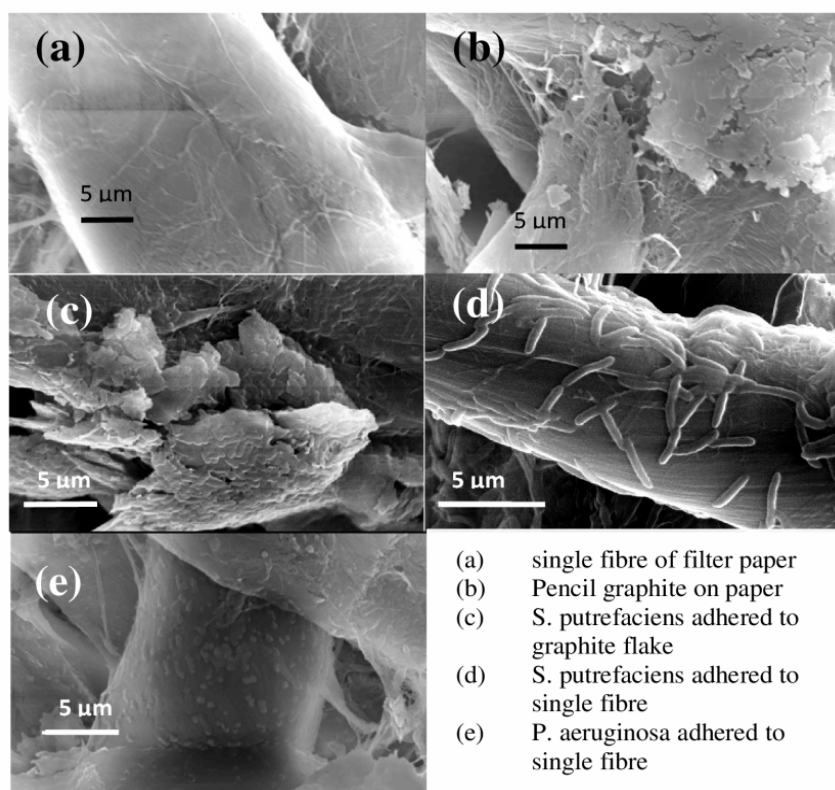


Figure S4: (a) Scanning electron micrograph of the Whatman no. 1 filter paper without any pre-treatment. (b) SEM image of the pencil stroked graphite electrodes over the paper matrix (c) *S. putrefaciens* adhered to graphite flakes facilitating direct electron transfer, (d) *S. putrefaciens*, adhered to integrated paper electrode (e) The presence of *P. aeruginosa* along the cellulosic fibres in the matrix

5. Cathode contamination

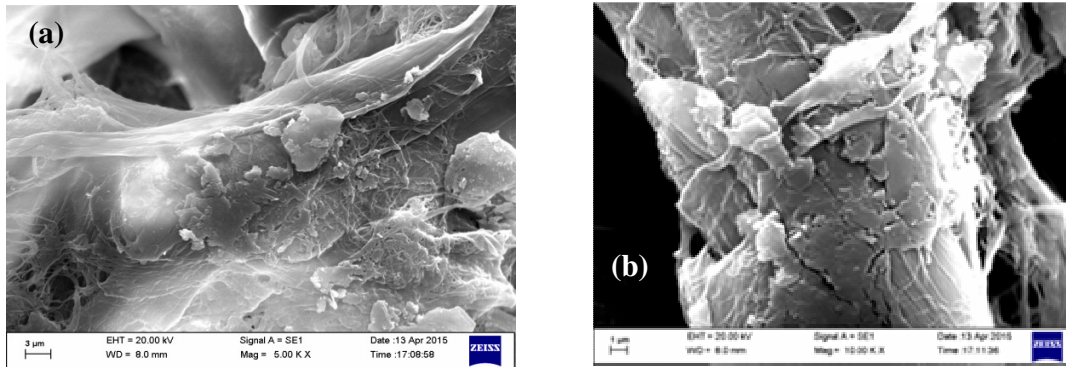


Figure S5: Scanning electron micrograph of the cathode (pencil stroked graphite) at (a) 5000X and (b) 10,000X showing the cellulosic fibers and the graphite deposited.

A double layered integrated paper electrode and two layers of separators are selectively adopted to prevent the bacterial contamination of the cathode. The graphite stroking further blocks the pores of the paper matrix and holds the bacteria. Further, to find if there is any contamination; SEM analysis of the cathode is done after the experimental run by injecting the bacteria at a concentration deployed in the study. The fibers are devoid of bacteria, indicating that cathode contamination is absent even at the end of the experimental run.

6. Effect of degassing

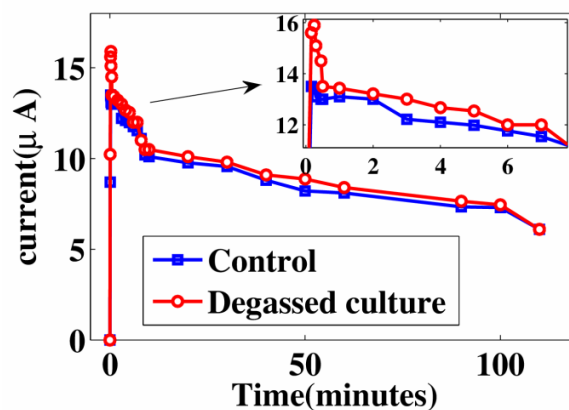


Figure S6: Current generation profiles for the organism *S. putrificiens* using degassed media.

Effect of degassing is studied by sparging sterile N_2 gas to ensure that the inherent dissolved oxygen is removed from the media. Equal volumes of both degassed and un-gassed (control) culture are injected in to the device and the current generation profiles of both are recorded with

time. Studies showed that, although there is an increase in the start-up values of the current, it soon dropped within 1 min to the value of control.

7. Effect of the surface area on the electricity production in the biofuel cell

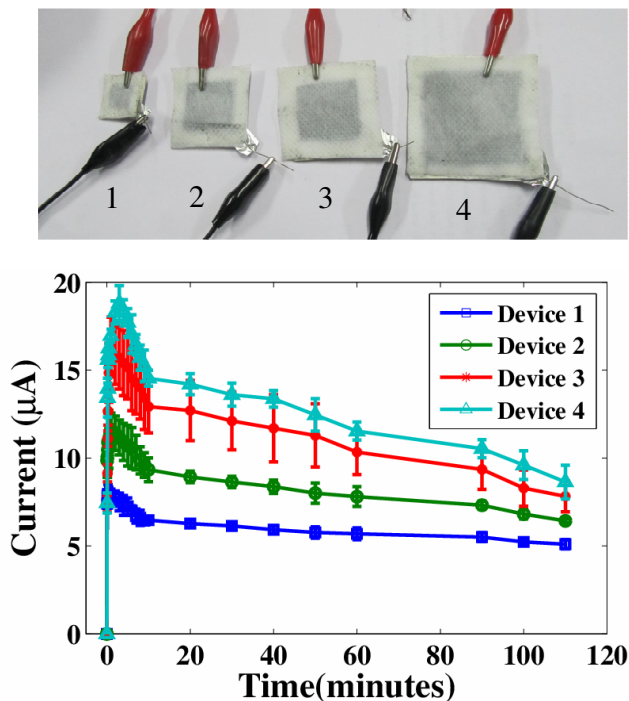


Figure S7: (a) Picture of the experimental set-ups with various surface areas and (b) Current generation profiles of the same.

S. No	Anode surface area (cm ²)	Cathode surface area (cm ²)	Volume of the culture injected (µL)
Device 1	1	4	100
Device 2	4	9	250
Device 3	9	16	400
Device 4	16	25	600

Table 1: Surface areas of the cathode and anode, along with the volumes of the culture injected for the different devices.

A scale down study has been carried out where the anode and cathode surface areas are varied and bacterial culture is injected accordingly as shown in Table 1. When the current generation profiles of each device are plotted, it is found that the Device 4 which has the maximum surface area produced the maximum current of 19 μA followed by Device 3, 2 and 1. This shows that power generation is proportional to the surface areas of the electrodes. One more important observation is that, there is a stable current generation in device 1 while the drop is significant when the surface area is increased, probably due to the enhancement of the evaporation rate across the cathode.

References:

1. M. Naebe, J. Wang, A. Amini, H. Khayyam, N. Hameed, L.H. Li, Y. Chen & B. Fox, “Mechanical Property and Structure of Covalent Functionalised Graphene/Epoxy Nanocomposites”, *Scientific Reports*, 2014, 4.
2. L. Lin, H. Yamaguchia and A. Suzukia, “Dissolution of cellulose in the mixed solvent of [bmim]Cl–DMAc and its application”, *RSC Adv.*, 2013,3, 14379-14384.
3. N. Lin, J. Huang and A. Dufresne, “Preparation, properties and applications of polysaccharide nanocrystals in advanced functional nanomaterials: a review”, *Nanoscale*, 2012, 4, 3274-3294.